RSC Advances

PAPER

View Article Online
View Journal | View Issue

Cite this: *RSC Adv.*, 2019, **9**, 40819

Synthesis of rotenone loaded zein nano-formulation for plant protection against pathogenic microbes†

Ngangom Bidyarani and Umesh Kumar *

Received 24th October 2019
Accepted 1st December 2019

DOI: 10.1039/c9ra08739g

rsc.li/rsc-advances

Rotenone (RN) is a naturally occurring isoflavone found in the root or rhizomes of fabaceae (a plant family), known for its insecticidal/pesticidal properties. Rotenone was loaded in zein nanoparticles (ZSC) by antisolvent precipitation method at room temperature. The synthesized nanoparticles showed self-assembled spherical nanostructures having 425.67 ± 7.02 and 471.33 ± 10.60 nm of hydrodynamic radii with −14.23 ± 0.21 and −17.64 ± 0.89 mV zeta potential for ZSC and RNZSC (rotenone loaded zein nanoparticles), respectively. The encapsulation of rotenone was confirmed by FTIR, ^{1}H NMR and DSC studies. A significant encapsulation efficiency of 95.82 ± 0.038% and 5.99 ± 0.002% loading efficiency were determined by HPLC studies. Synthesized RNZSC showed excellent antimicrobial activity against plant pathogens- *P. syringae* and *F. oxysporum*. Our studies showed for the first time direct evidence of antimicrobial activity of rotenone against plant pathogens. A similar approach could be adopted for developing several new botanical based nano-formulations with their known insecticidal effect, to control certain plant diseases in an environment friendly and sustainable manner.

1. Introduction

Rotenone is a natural active ingredient with broad insecticidal and a few acaricidal properties, derived from the roots or rhizomes of several tropical plants such as *Derris*, *Amorpha*, *Lonchocarpus* and *Tephrosia*.[1] The root and stem part of *D. scandens* were reported as showing good antibacterial, antifungal and antialgal properties[2] but rotenone was not mentioned as a responsible factor in these previous studies. It has been used for its broad-spectrum insecticidal property to control aphids, suckers, acari and insects infecting fruits and vegetables.[3] Rotenone has been allowed to be used in organic farming because of its plant origin, being easily degradable, harmless to non-target organisms and having low resistance development attributes.[4] As reported in the pesticide information profile of the extension toxicological network (extoxnet),[5] rotenone is highly photosensitive and also sensitive to heat and high temperature. Rotenone readily degraded in soil and water and its half-life degradation time (DT_{50}) in these environments is within 3–6 days.[6] However, the application of rotenone in agricultural sector was restricted due to its poor solubility in water (0.002 mg mL^{-1}), thus needs to be dissolved in polar solvents.[4,7,8] Additionally, excessive use of organic solvents has significantly contaminated the environment.[9,10]

The ever increasing, human population has imposed significant pressure on agriculture to increase yield with limited resources which has led to the enormous increase in development of antimicrobial and insecticidal nano-formulations for controlling plant diseases and pests. The use of different matrices, including biodegradable polymers, lipids, proteins, among others, as carrier agents for targeted delivery of active ingredients toward controlling plant diseases, insects and pests have shown great promises.[11–13]

Zein is a corn prolamine, rich in amino acids such as proline, leucine, glutamine and alanine. Hydrophobicity makes zein capable of self-association in presence of polar solvents, water, which has already been used to encapsulate essential oils, including oregano, thyme, thymol, curcumin and carvacrol.[14,15] Zein act as a promising agent to develop various nano-formulations since it is biocompatible, biodegradable, less toxic and cost effective.[16,17] Sodium caseinate (SC) is a blend of different caseins. It acts as both natural emulsifier and stabilizer consisting different hydrophilic and hydrophobic moieties.[18] Zein and SC are generally regarded as safe (GRAS) by the Food and Drug Administration (FDA). However, encapsulation of rotenone (RN) in zein using SC has never been reported yet.

In the present study, a zein based biodegradable nano-formulation was prepared to deliver rotenone and evaluated its potency against plant pathogenic microbes, *P. syringae* and *F. oxysporum*. The prepared nano-formulation could be used to control plant pathogenic microorganisms, hence contributing to the goal of sustainable agriculture.

School of Nano Sciences, Central University of Gujarat, Gandhinagar 382030, Gujarat, India. E-mail: umesh.kumar@cug.ac.in

† Electronic supplementary information (ESI) available. See DOI: 10.1039/c9ra08739g

2. Materials and methods

2.1 Materials

Zein (Z 3625; CAS number: 9010-66-6) and rotenone (R8875; ≥95%; CAS number 83-79-4) were purchased from Sigma Aldrich. Sodium caseinate (SC) was obtained from SRL. Ethanol was acquired from Bioscience laboratory. Milli Q water was used throughout the experimental work. Nutrient agar (NA), potato dextrose agar (PDA), nutrient broth (NB), potato dextrose broth (PDB) were obtained from Himedia laboratories. *Pseudomonas syringae* was obtained from Junagadh Agricultural University and *Fusarium oxysporum* was purchased from division of plant pathology, IARI, New Delhi. All the solvents and chemicals used were of analytical grade. Syringe filter was obtained from Axiva.

2.2 Preparation of zein nanoparticles and rotenone loaded zein nanoparticles using SC

Zein nanoparticles using SC were prepared by antisolvent precipitation with slight modification.[19] Zein was dissolved in aqueous ethanol solution of 85% (v/v) and stirred overnight at room temperature (25 °C). The prepared zein solution was filtered through 0.45 μm syringe filter. Rotenone solution was prepared (3.33 μg μL^{-1}) in absolute ethanol. SC solution (500 μg mL^{-1}) was prepared in Milli Q water and mixed with the prepared zein solution (1 mg mL^{-1}) under continuous magnetic stirring to obtain a homogenous colloidal suspension (ZSC). For the loading of rotenone, 100 μg mL^{-1} of rotenone solution was mixed with prepared zein solution and precipitated with water containing SC under continuous magnetic stirring at 500 rpm for 4 h at 25 °C, resulting in the formation of stable colloidal suspension (RNZSC). The prepared colloidal suspension was freeze dried for 24 h and used for further physicochemical and morphological characterizations using different techniques.

2.3 Physicochemical characterization of the prepared zein nanoparticles

2.3.1 Ultra-violet visible spectroscopy. The freshly prepared zein nanoparticles using SC (ZSC), zein solution (zein), pure rotenone (RN) and rotenone loaded zein nanoparticles (RNZSC) were characterised using UV-1800, Shimadzu UV spectrophotometer. These samples were dispersed in water and scanned in the range of 500–200 nm to record its absorbance at room temperature.

2.3.2 Dynamic light scattering (DLS). The freshly prepared nanoparticles, ZSC and RNZSC, were taken for DLS measurement. 200 μL of the prepared nanoparticles were dispersed in Milli-Q water making final volume of 2 mL and then the colloidal solution was sonicated for 10 minutes. The well dispersed colloidal solutions were investigated for particle size, poly dispersity index (PDI) and zeta potential by Metrohm DLS instrument. The samples were prepared at 25 °C and signals with a backscattering angle of 173° were captured for data generation. All measurements of the samples were taken in triplicate.

2.3.3 Field emission scanning electron microscopy (FE-SEM). The morphology of the prepared rotenone loaded (RNZSC) and unloaded zein NPs (ZSC) were characterized using FESEM (JEOL, JSM7600F). The deposited samples on aluminum foil were sputter coated with gold–palladium mixture under vacuum for 5 minutes and were evaluated by FESEM, operated at an accelerating voltage of 10 kV.

2.3.4 Fourier transform infrared spectroscopy (FTIR). FTIR (PerkinElmer Spectrum 65) analyses were performed to determine the presence of various functional groups in pure rotenone (RN), previously lyophilized RNZSC and ZSC nanoparticles. The analysis was carried out with over 64 cumulative scans in the wavenumber between 4000 and 400 cm^{-1}, with 4 cm^{-1} resolution.

2.3.5 Proton nuclear magnetic resonance spectroscopy (^{1}H NMR) analysis. The ^{1}H NMR spectroscopy, Bruker 500 MHz Ultra shield plus NMR instrument was used to identify the types of hydrogen bond present in pure RN, pure zein powder (zein), previously lyophilized ZSC and RNZSC. Approximately 5 mg of each sample was dissolved in deuterated chloroform ($CDCl_3$). The ^{1}H NMR analysis was carried out at 298 K and at frequency of 500 MHz.

2.3.6 Differential scanning calorimeter (DSC). DSC (PerkinElmer, DSC 6000) was used to evaluate the thermal degradation and shifts, if any, in the peaks of ZSC, RNZSC and RN. Approximately 5 mg of each sample (previously lyophilized) was weighed. The samples were heated in an aluminium pan at the heating rate of 10 °C min^{-1}, with 20 mL min^{-1} nitrogen flow. The samples were analysed at temperatures between 55 to 210 °C. An empty sealed aluminium pan was used as baseline.

2.3.7 High performance liquid chromatography (HPLC): measurement of rotenone content in zein nanoparticles NPs with SC. The freshly prepared RNZSC was centrifuged at 10 000 rpm for 10 minutes at 4 °C to quantify the amount of rotenone. The amount of free rotenone in the collected supernatant was measured using Jasco Quaternary; Ultra Test HPLC-4000. The mobile phase in the analysis was consist of acetonitrile and deionised water in the volume ratio 80 : 20. The chromatogram was detected at 298 nm using a UV detector.

The encapsulation efficiency (EE) and loading efficiency (LE) were calculated using the eqn (1) and (2), respectively.

$$\%\ \mathrm{EE} = \frac{\text{Total amount of rotenone loaded} - \text{free rotenone}}{\text{Total amount of rotenone loaded}} \times 100 \quad (1)$$

$$\%\ \mathrm{LE} = \frac{\text{Total amount of rotenone loaded} - \text{free rotenone}}{\text{Total amount of carrier}} \times 100 \quad (2)$$

2.3.8 Antimicrobial activity. Antimicrobial activity of the prepared ZSC, RNZSC and pure rotenone (RN) were performed in 96-well microplate using a Biotek synergy hybrid microplate reader. The pure RN is dissolved in ethanol and further diluted in water to obtain the same concentration of RNZSC. Before the antimicrobial assay, the *P. syringae* strain was grown on nutrient

agar (NA) and nutrient broth (NB). The *F. oxysporum* was also sub cultured on potato dextrose agar (PDA) and then grown in potato dextrose broth (PDB) for the antifungal assay.

The bacterial suspension of *P. syringae* was adjusted to achieve an optical density of about 0.6 (a.u.) at 600 nm (OD_{600}), which is approximately 1×10^6 to 10^7 cfu mL^{-1}, and then diluted further to achieve 1×10^5 to 10^6 cfu mL^{-1}.[19] For the antibacterial assay, 100 μL of diluted suspension (*P. syringae*) was taken in each well. Then mixed with prepared ZSC, RNZSC and RN at various concentrations (4–20 μg mL^{-1}) in each well of 96-well microplate. The final volume was made up to 250 μL with nutrient broth (NB) in each well of the 96-well microplate. *P. syringae* suspensions without adding any samples (RN, RNZSC and ZSC) was kept as negative control (NC as included in Fig. 6). Minimum inhibitory concentration (MIC) value of RNZSC was determined by broth dilution method with some modifications.[19,20] The microplate which contained *P. syringae* suspension with and without ZSC, RN and RNZSC was incubated at 28 °C for 24 h. The measurement for antibacterial activity against *P. syringae* was taken at 600 nm from 0 h to 24 h at different time interval using a Biotek synergy hybrid microplate reader. The plate assay of the antibacterial activity is given in Fig. S2, ESI.†

For antifungal assay, spore of *F. oxysporum* grown in PDA was scraped and then dissolved in distilled water to prepare its suspension. Absorbance of the prepared spore suspension was taken until 0.6 (a.u.) was achieved at 595 nm which corresponds to nearly 2000 spores or mycelial fragments.[21] Pure RN was prepared as mentioned in antibacterial assay. 30–150 μL of RN, RNZSC, and ZSC were added in each well for the antifungal assay. The added volume corresponds to the concentration ranging from 12–60 μg mL^{-1} for pure RN and RNZSC. 10 μL of prepared spore suspension (*F. oxysporum*, 0.6 $OD_{595\ nm}$ determined) was added in each well. The total volume of each well was made up to 250 μL by adding PDB. Spore suspensions of *F. oxysporum* without adding any samples (RN, RNZSC and ZSC) was kept as negative control (NC as included in Fig. 7). The microplate which contained spore suspension of *F. oxysporum* with and without RN, RNZSC and ZSC was incubated at 28 °C for 120 h (5 days). Measurement for studying the antifungal activity against *F. oxysporum* was taken for every 24 h till 120 h at 595 nm using a Biotek synergy hybrid microplate reader. Each sample was prepared in triplicate for antibacterial and antifungal assay.

3. Results and discussion

3.1 UV-visible spectroscopy of the prepared nanoparticles

The UV visible spectra of prepared samples, ZSC, RNZSC, RN and the zein solution (zein) were recorded in the range from 200 to 500 nm (Fig. 1). In the spectra, it is clearly observed that a prominent peak was appeared around 277 nm indicating the characteristic absorbance pattern for pure zein, due to the presence of aromatic amino acids.[22] Further, absorption spectra were recorded for the zein nanoparticles prepared using SC (ZSC) by antisolvent precipitation method. A broader peak was observed in ZSC at 356 nm with the 79 nm red shift compared to

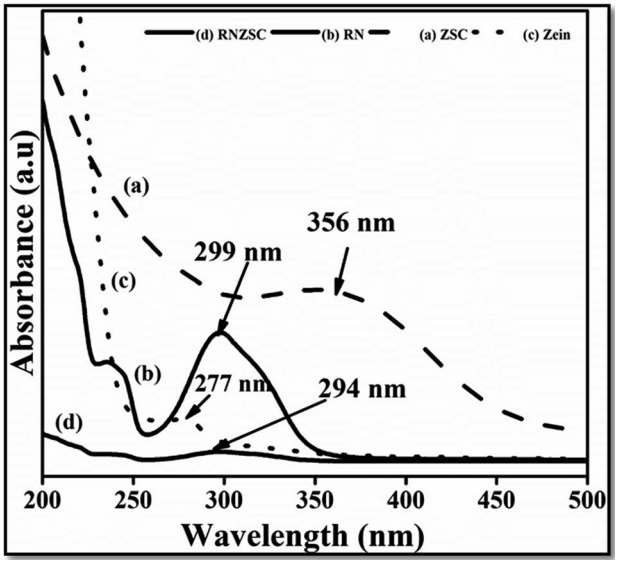

Fig. 1 UV-visible spectra of (a) ZSC, (b) RN, (c) zein, and (d) RNZSC.

the pure zein, indicating electrostatic interaction of SC with zein nanostructures. Additionally, pure rotenone (RN) showed 299 nm absorption peak,[23] which is slightly shifted in case of rotenone loaded zein nanoparticles (RNZSC). The absorbance at ~240 nm was observed in case of RN and RNZD due to detection of rotenoids[24] and rotenone is the prototypical member of its family.

3.2 Fourier transform infrared spectroscopy of the prepared nanoparticles

The infrared spectroscopy (FTIR) was used to investigate the chemical interaction of rotenone with zein nanoparticles in terms of frequency change in vibrational stretching modes. The FTIR analysis were performed for pure rotenone (RN), rotenone loaded zein nanoparticles (RNZSC) and zein nanoparticles (ZSC) at room temperature (25 °C). The FTIR spectrum of ZSC shows an intense band between 1644, 1545 and 2928 cm^{-1} attributed to amides I, II along with = CH_2, C–H stretching of zein protein[17] as shown in Fig. 2. In the FTIR spectrum, the peaks around 2938, 1674, 1605, 1515, 1456, 1357 and 1091 cm^{-1} are relevant to C–H, C=O, C–O and C=C stretching frequencies of the cyclic alkene which is present in pure rotenone structures.[9,25,26] The peaks around 2938 cm^{-1} contributed to the C–H bending of aromatic alkyl which may be attributed to the characteristic peak of pure rotenone which were found around 2968 cm^{-1} in case of RNZSC.[27,28] Based on spectral changes in alkyl groups and increased in the intensity of characteristic bands at 2968, 1663, 1535, 1458, 1359 and 1093 cm^{-1} frequencies, it can be concluded that the rotenone was successfully loaded on zein nanoparticles (RNZSC). In the FTIR spectra, no new bands were found after encapsulation of rotenone in zein nanoparticles which may be due to the physical interactions of the prepared rotenone loaded nanoparticles rather than stronger chemical bonds which were similar with the findings reported earlier.[15,17]

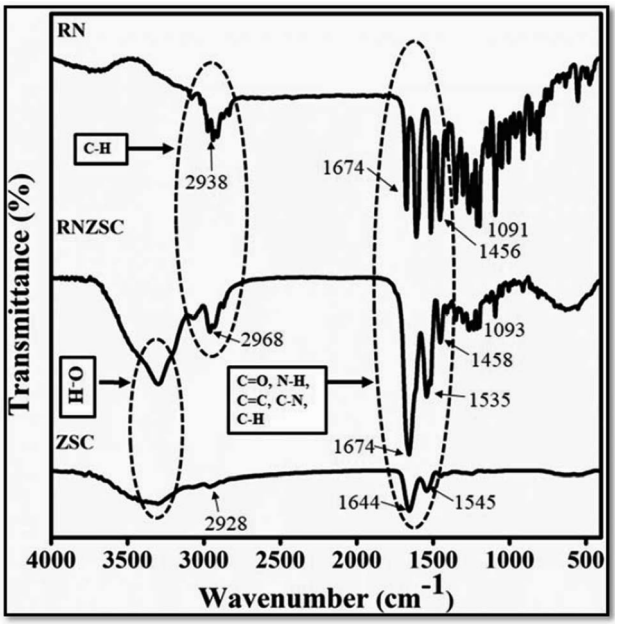

Fig. 2 FTIR spectra of pure rotenone (RN), rotenone loaded zein NPs (RNZSC) and unloaded zein NPs (ZSC).

3.3 Differential scanning calorimetry (DSC) study of the prepared nanoparticles

The thermal properties of prepared zein nanoparticles with SC (ZSC), rotenone loaded zein nanoparticles with SC (RNZSC) and pure rotenone (RN) were analyzed using DSC. The DSC thermograms for all the samples are shown in Fig. 3 in the range of (55 to 210) °C. The DSC thermograms of ZSC exhibited a broad peak at 72 °C which is an endothermic thermal character. The RNZSC showed a broad endothermic peak at 66 °C may be due to the weight loss of hydrocarbons in the combined phase[19] with a minor endothermic peak around 157 °C. Further, the pure RN exhibited a sharp endothermic peak at 164 °C. This temperature shifting and lack of sharp endothermic peak in RNZSC as compared to pure RN, suggested the uniform dispersion and encapsulation of RN in RNZSC. Similar results were also reported previously, where absence of endothermic peak in DSC confirms the molecular dispersion and encapsulation of VD3 in zein/carboxymethyl chitosan (CMCS) nanoparticles.[29]

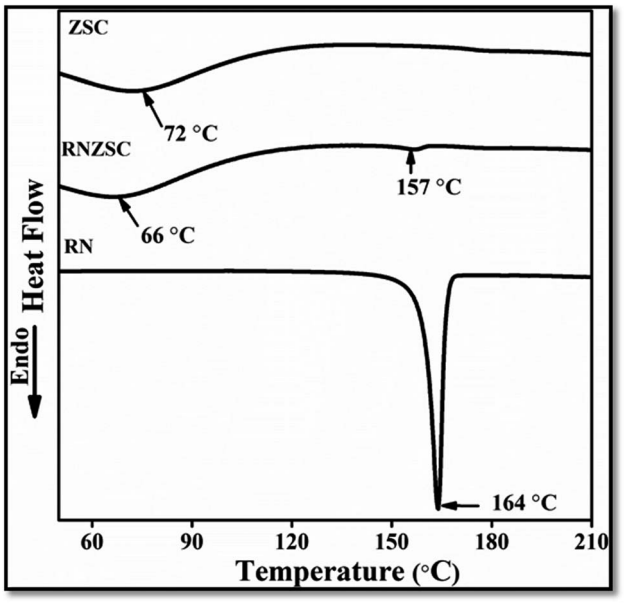

Fig. 3 Thermal studies of unloaded zein nanoparticles (ZSC), rotenone loaded (RNZSC) and free rotenone (RN) by DSC.

3.4 Field emission scanning electron microscope analysis of the prepared nanoparticles

The morphological study by FE-SEM is carried out for the synthesized zein nanoparticles (ZSC) and rotenone loaded zein nanoparticles (RNZSC) showed in Fig. 4(a) and (b) respectively. The micrographs showed a spherical shape with the self-assembled structures for both the samples.[29,30] The self-assembled nature of the prepared nanospheres are due to the amphiphilic nature of the zein molecules which induces a driving force for self-assembly.[31,32] Further, SC has been used as emulsifier to stabilize the hydrophobic part of zein structure causing a repulsive electrostatic and steric hindrances to prevent agglomeration, creating the hydration properties of the prepared nanoparticles.[33–35] Both samples showed spherical shape and smooth surfaces, due to the adsorption of SC on zein surfaces by electrostatic force. It is interesting to note that rotenone loaded zein nanoparticles showed well dispersed nanoparticles with larger particle size while the unloaded zein nanoparticles showed cross linked nanoparticles with unequal distribution of particle size. The histogram for the average size of ZSC and RNZSC is provided in ESI (Fig. S4†). The average sizes calculated from FE-SEM micrographs for ZSC and RNZSC are 324.85 and 467 nm, respectively (Fig. S4†). The deposition of rotenone in zein nanoparticles which probably blocks the adsorption of SC may increase the hydrophobic interaction induced aggregation behavior in RNZSC thus resulting in its increased size, compared to ZSC.[36] Here, sizes are found more than 100 nm which are in consistent with our DLS results. There are previous literature reports where sizes with 200 nm (ref. 37) and 300 nm (ref. 38) particles are termed as nanoparticles. The better distribution of the RNZSC could be due to the steric repulsion and hydrophobic interaction.[30] Rotenone is a hydrophobic botanical and is successfully encapsulated in the synthesized zein nanoparticles confirmed by our FTIR (Fig. 2) and DSC (Fig. 3) studies.

3.5 Nuclear magnetic resonance (NMR) analysis of the synthesized nanoparticles

The presence of rotenone in synthesized zein nanoparticles with SC was also investigated by ^{1}H NMR spectroscopy. The spectrum of pure rotenone (RN) showed ^{1}H NMR signal peaks at 7.9–6.5 (H of aromatic ring), 5.3–5.0 (H attached to alkene C=CH), 4.6–2.9 (H of –O–CH–), 2.1 (CH_3–CO), 1.9–1.7 (–CH_2–).[9,39] The signal peaks at δ 2.2 (–CH of –NH), 1.6–1.3 (–CH_2–) are observed in pure zein powder spectrum. The spectrum of zein

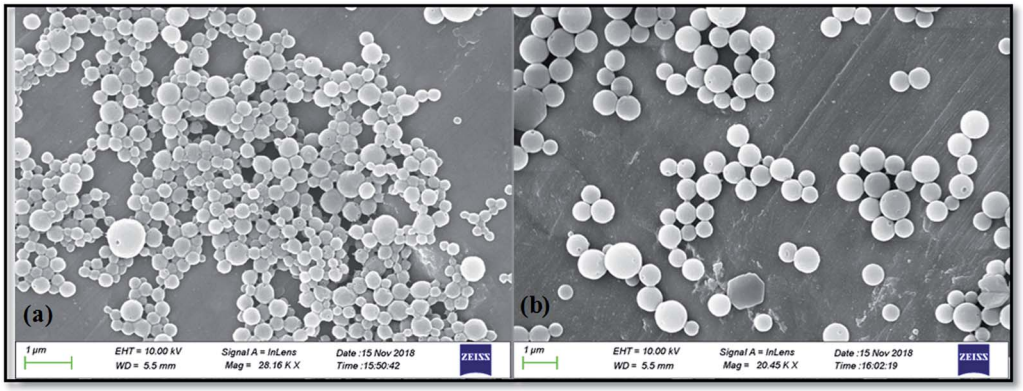

Fig. 4 FE-SEM micrographs of (a) ZSC and (b) RNZSC.

nanoparticles with SC (ZSC) gave signal peaks at δ 3.9 (–O–CH_2– of SC), 2.2–1.8 (–CH of –NH of zein) and 1.6–1.4 (–CH_2– of zein) which are attributed to both zein and sodium caseinate (SC). RNZSC nanoparticles gave ^{1}H NMR signal peaks at δ 7.9–6.6 (H of aromatic ring), 5.3–4.9 (H attached to alkene C=CH), 4.6–4.3 (H of –O–CH–), 3.8 (–O–CH_2– of SC), 2.2 (CH_3–CO), 1.8–1.6 (–CH_2– of RN; –CH of –NH of SC and –CH_2– of zein), and 1.3 (–CH_2– zein) which are also present in respective spectra of RN and ZSC individually.[40] The RNZSC NPs showed the ^{1}H-NMR signature peaks of both RN and ZSC. In RN loaded ZSC NPs ^{1}H-NMR spectra showed the δ values which are slightly shifted as $\pm$0.1 ppm, this may be due to hydrophobic interaction and hydrogen bonding but no covalent bond between RN and ZSC (Fig. 5 and Table ST1, ESI†). Hence, the observed results suggested the successful encapsulation of rotenone in zein NPs.

3.6 Study of size distribution, encapsulation and loading efficiency of rotenone loaded and ZSC

The particle size, distribution pattern and the zeta potential of zein nanoparticles (ZSC) and rotenone loaded zein nanoparticles (RNZSC) were determined using DLS. The encapsulation efficiency (EE) and loading efficiency (LE) were also measured using HPLC technique and the obtained parameters are tabulated in Table 1. DLS studies showed hydrodynamic sizes of 425.67 $\pm$ 7.02 nm and 471.33 $\pm$ 10.60 nm for the ZSC and RNZSC nanoparticles with 0.78 $\pm$ 0.10 and 0.64 $\pm$ 0.01 PDI value, respectively. DLS graph for size with zeta potential profile is shown in ESI (Fig. S3†). The particle size of the rotenone loaded is higher as compared to the unloaded, due to the hydrophobic interaction between the zein carrier and the loaded rotenone leading to more stable and self-assembled monodispersed (PDI < 1) colloidal nanoparticles.[9,17,30,41] The PDI values obtained were <1, indicating the uniform distribution avoiding agglomeration due to presence of SC emulsifier in the prepared nanoparticles. However, -14.23 ± 0.21 and -17.64 ± 0.89 mV zeta potential were recorded for unloaded and RN loaded zein nanoparticles (ZSC and RNZSC) respectively. The zeta potential values also agreed for the better stability of the rotenone loaded nanoparticles which is in accordance with our FE-SEM data. The rotenone loaded nanoparticles remained stable for the longer period, mainly due to the steric stabilization provided by the botanical, rotenone.[17]

The amount of rotenone loaded in the prepared nanoparticles was quantified using HPLC technique through which we calculated the encapsulation efficiency (EE%) and loading efficiency (LE%), shown in Table 1. An encapsulation efficiency (EE%) of 95.82 $\pm$ 0.038% and loading efficiency (LE%) of 5.99 $\pm$ 0.002% were recorded for the RNZSC which is higher than the percentage of rotenone determined and reported by previous

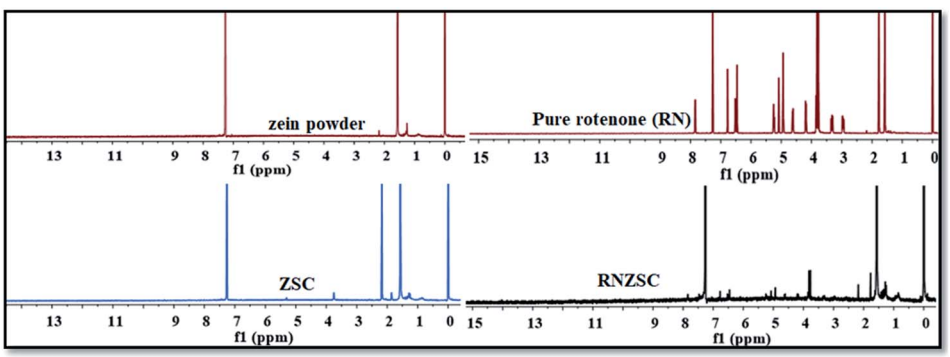

Fig. 5 Chemical shift analysis of pure zein powder, zein nanoparticles (ZSC), rotenone loaded zein nanoparticles (RNZSC) and pure rotenone (RN) by ^{1}H NMR spectra.

Table 1 Size, zeta potential, PDI, EE and LE from DLS and HPLC of unloaded (ZSC) and rotenone loaded (RNZSC) zein nanoparticles with SC[a]

Samples	Size (nm)	Zeta potential (mV)	PDI	EE%	LE%
ZSC	425.67 ± 7.02	−14.23 ± 0.21	0.78 ± 0.10	—	—
RNZSC	471.33 ± 10.60	−17.64 ± 0.89	0.64 ± 0.01	95.82 ± 0.038	5.99 ± 0.002

[a] ± values are considered in triplicate measurements.

studies.[28,39] Similarly, high encapsulation efficiencies of essential oils were also reported in zein nanoparticles.[19] Botanical repellants, geraniol and citronellal were reported with >90% EE% in zein nanoparticles formulation.[17] However, in our study, we reported the first-time encapsulation of rotenone in zein nanoparticles with SC. The increased in EE% and LE% as compared to other reported polymeric micelles/nanoparticles could be due to the enhanced hydrophobic interaction between rotenone and zein nanoparticles stabilized with SC which lead to the promotion of more space for rotenone to be entrapped in the hydrophobic core of spherical colloidal nanoparticles.

3.7 Antimicrobial activity

The antibacterial and antifungal efficacy of rotenone (RN), rotenone loaded zein nanoparticles (RNZSC) and zein nanoparticles (ZSC) were evaluated by *in vitro* study and the results are shown in Fig. 6 and 7. The plate assay for the antifungal and antibacterial activity are also provided in the ESI (Fig. S1 and S2†). Antibacterial studies of RNZSC showed minimum inhibitory concentration (MIC) at 16 μg mL^{-1} against *P. syringae*.

While, antifungal studies of RNZSC showed MIC at 48 μg mL^{-1} against *F. oxysporum*. Rotenone is a broad spectrum insecticide which is a constituent of the root part of *D. scandens* and the antimicrobial activity of *D. scandens* extract have been reported previously against *E. coli, B. megaterium*, *C. fusca* and *M. violaceum*[2] but none of these previous studies has reported that rotenone is a responsible factor for its antimicrobial activity.

In our study, equal concentration of *P. syringae* suspension (100 μL corresponding to 1×10^5 to 10^6 cfu mL^{-1}) were taken in each well for antibacterial activity. Similarly, we have taken equal number of fungal spores (2000) in each well for antifungal activity. RNZSC showed better antibacterial activity against Gram negative plant pathogenic bacteria *P. syringae* compared to RN and ZSC which is shown in Fig. 6 and S2 (ESI†). Additionally, antifungal activity of the prepared samples, RNZSC, RN and ZSC against *F. oxysporum* were investigated for 120 h (5 days) and the measurement was taken after every 24 h because the log phase of *F. oxysporum* was observed at third day (72 h) after inoculation. It was evaluated that the RNZSC showed the better antifungal activity as compared to RN and ZSC, depicted in Fig. 7 and S1 (ESI†). Rotenone inhibit the oxygen uptake and

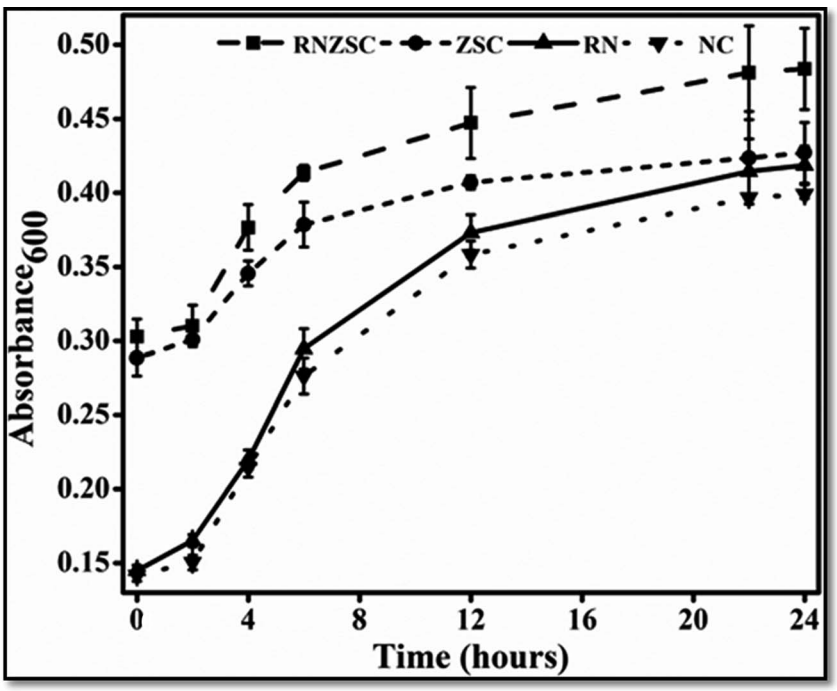

Fig. 6 Antibacterial activity of RNZSC, ZSC, RN and NC against *P. syringae*. Negative control (NC) represents the absorbance of the suspension of *P. syringae* without adding any nanoparticles. Error bars indicate the standard deviations from three replicates.

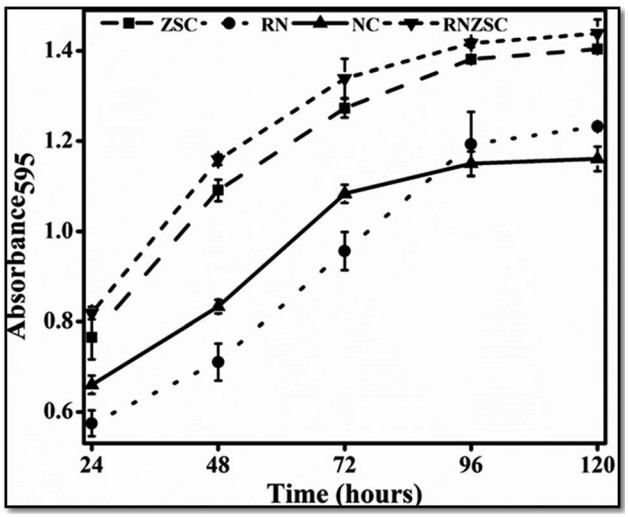

Fig. 7 Antifungal activity of RNZSC, ZSC, RN and NC against *F. oxysporum*. Negative control (NC) represents the absorbance of the spore suspension of *F. oxysporum* without adding any nanoparticles. Error bars indicate the standard deviations from three replicates.

also block the electron transport chain (ETC)[42] leading to the cessation of microbial growth which could be the reason for showing antimicrobial activity against *P. syringae* and *F. oxysporum*. Rotenone has been allowed to use in organic farming because of its plant origin, easily degradable, harmless to non-target organisms and low resistance development attributes.[4] Besides this, rotenone readily degrades in soil and water and its half-life (DT_{50}) in these environments is 3–6 days. The loaded rotenone concentration (100 μg mL^{-1}) is much lower than the reported oral lethal dose (LD_{50}) of rotenone which ranges from 132–1500 mg kg^{-1} in rats and 300–500 mg kg^{-1} in humans.[5] Rotenone is a known insecticidal agent but its antimicrobial activity as direct evidence was demonstrated by our studies for the first time.

4. Conclusion

A spherical self-assembled colloidal zein nanoparticles loaded with rotenone using SC were successfully synthesized using antisolvent precipitation method. DLS studies showed hydrodynamic sizes measured around 425.67 ± 7.02 nm and 471.33 ± 10.60 nm for ZSC and RNZSC respectively. The FTIR peaks assigned at 1091, 1663 and 2968 cm^{-1} are attributed to the carbonyl group, cyclic alkene and amide group stretching of both rotenone and zein and also the signal peaks of ^1H NMR which observed at 1.8, 3.8, 6.5 and 7.9 ppm correspond to –O–CH_2– and H of aromatic ring in both zein and rotenone have confirmed the successful encapsulation of rotenone in the synthesized zein nanoparticles due to hydrogen bonding and hydrophobic interaction. The DSC has confirmed the encapsulation of rotenone in the prepared zein nanoparticles in terms of lack of sharp endothermic peak and temperature shifts. The EE of 95.82 ± 0.038% and LE 5.99 ± 0.002% were determined by HPLC for the synthesized rotenone loaded zein nanoparticles (RNZSC). The prepared RNZSC showed excellent antimicrobial activity against plant pathogens, *i.e. P. syringae* and *F. oxysporum*. The efficiency of the prepared nano-formulation needs to be evaluated at large scale for field trial studies and such carrier needs to be further studied for its suitability for other type of botanicals or active ingredients (AIs). These findings from our study will open several new possibilities to control certain plant diseases in an environmentally friendly and sustainable manner.

Conflicts of interest

There are no conflicts to declare.

Acknowledgements

Ngangom Bidyarani would like to thank University Grant Commission (UGC) for providing non-net financial support and Central University of Gujarat for allowing accessibility to Central Instrumentation Facility (CIF-CUG) to complete this research work.

References

1 L. Crombie and D. A. Whiting, *Phytochemistry*, 1998, **49**, 1479–1507.
2 H. Hussain, A. Al-Harrasi, K. Krohn, S. F. Kouam, G. Abbas, A. Shah, M. A. Raees, R. Ullah, S. Aziz and B. Schulz, *J. King Saud Univ., Sci.*, 2015, **27**, 375–378.
3 M. B. Isman, *Annu. Rev. Entomol.*, 2005, **51**, 45–66.
4 S.-B. Lao, Z.-X. Zhang, H.-H. Xu and G.-B. Jiang, *Carbohydr. Polym.*, 2010, **82**, 1136–1142.
5 Extoxnet, http://pmep.cce.cornell.edu/profiles/extoxnet/pyrethrins-ziram/rotenone-ext.html#14.
6 I. Cavoski, P. Caboni, G. Sarais and T. Miano, *J. Agric. Food Chem.*, 2008, **56**, 8066–8073.
7 X.-J. Chen, H.-H. Xu, W. Yang and S.-Z. Liu, *J. Photochem. Photobiol., B*, 2009, **95**, 93–100.
8 L. Martin, S. Liparoti, G. Della Porta, R. Adami, J. L. Marqués, J. S. Urieta, A. M. Mainar and E. Reverchon, *J. Supercrit. Fluids*, 2013, **81**, 48–54.
9 M. Kah and T. Hofmann, *Environ. Int.*, 2014, **63**, 224–235.
10 H. Fessi, F. Puisieux, J. P. Devissaguet, N. Ammoury and S. Benita, *Int. J. Pharm.*, 1989, **55**, R1–R4.
11 K. Ding, L. Shi, L. Zhang, T. Zeng, Y. Yin and Y. Yi, *Polym. Chem.*, 2016, **7**, 899–904.
12 A. Lucia, A. C. Toloza, E. Guzmán, F. Ortega and R. G. Rubio, *PeerJ*, 2017, **5**, e3171.
13 N. Parris, P. H. Cooke and K. B. Hicks, *J. Agric. Food Chem.*, 2005, **53**, 4788–4792.
14 Y. Wu, Y. Luo and Q. Wang, *LWT–Food Sci. Technol.*, 2012, **48**, 283–290.
15 R. Paliwal and S. Palakurthi, *J. Controlled Release*, 2014, **189**, 108–122.
16 J. L. de Oliveira, E. V. R. Campos, A. E. S. Pereira, T. Pasquoto, R. Lima, R. Grillo, D. J. de Andrade, F. A. dos

Santos and L. F. Fraceto, *J. Agric. Food Chem.*, 2018, **66**, 1330–1340.
17 F. Li, Y. Chen, S. Liu, J. Qi, W. Wang, C. Wang, R. Zhong, Z. Chen, X. Li, Y. Guan, W. Kong and Y. Zhang, *Int. J. Nanomed.*, 2017, **12**, 8197–8209.
18 S. Zhang and Y. Han, *PLoS One*, 2018, **13**, e0194951.
19 Y. Zhang, Y. Niu, Y. Luo, M. Ge, T. Yang, L. Yu and Q. Wang, *Food Chem.*, 2014, **142**, 269–275.
20 N. S. Weerakkody, N. Caffin, M. S. Turner and G. A. Dykes, *Food Control*, 2010, **21**, 1408–1414.
21 W. F. Broekaert, F. R. G. Terras, B. P. A. Cammue and J. Vanderleyden, *FEMS Microbiol. Lett.*, 1990, **69**, 55–59.
22 R. Girija Aswathy, B. Sivakumar, D. Brahatheeswaran, T. Fukuda, Y. Yoshida, T. Maekawa and D. Sakthi Kumar, *Adv. Nat. Sci.: Nanosci. Nanotechnol.*, 2012, **3**, 25006.
23 M. Yang, Y. Chen, J. Liu, J. Ma and L. Huai, *J. Anal. Chem.*, 2011, **66**, 820.
24 X.-N. Zeng, J. Coll, S.-X. Zhang, X.-Q. Liu and F. Camps, *Chin. J. Chromatogr.*, 2002, **20**, 144–147.
25 M. Prabaharan, R. L. Reis and J. F. Mano, *React. Funct. Polym.*, 2007, **67**, 43–52.
26 B. Feng, M. A. Ashraf and L. Peng, *Open Life Sci.*, 2016, **11**, 380.
27 N. F. A. Aljafree and A. Kamari, *J. Polym. Res.*, 2018, **25**, 133.
28 S. N. M. Yusoff and A. Kamari, *J. Appl. Polym. Sci.*, 2018, **135**, 46855.
29 Y. Luo, Z. Teng and Q. Wang, *J. Agric. Food Chem.*, 2012, **60**, 836–843.
30 L. Wang and Y. Zhang, *J. Agric. Food Chem.*, 2017, **65**, 2990–2998.
31 D. W. P. M. Löwik and J. C. M. van Hest, *Chem. Soc. Rev.*, 2004, **33**, 234–245.
32 P. Nonthanum, Y. Lee and G. W. Padua, *J. Cereal Sci.*, 2013, **58**, 76–81.
33 H. Chen, Y. Zhang and Q. Zhong, *J. Food Eng.*, 2015, **144**, 93–102.
34 A. R. Patel, E. C. M. Bouwens and K. P. Velikov, *J. Agric. Food Chem.*, 2010, **58**, 12497–12503.
35 H. Liang, B. Zhou, L. He, Y. An, L. Lin, Y. Li, S. Liu, Y. Chen and B. Li, *RSC Adv.*, 2015, **5**, 13891–13900.
36 K. K. Li, S. W. Yin, Y. C. Yin, C. H. Tang, X. Q. Yang and S. H. Wen, *J. Food Eng.*, 2013, **119**, 343–352.
37 K. Jiang, D. Xu, Z. Liu, W. Zhao, H. Ji, J. Zhang, M. Li, T. Zheng and H. Feng, *RSC Adv.*, 2019, 37292–37299.
38 L. An, D. Zhang, L. Zhang and G. Feng, *Nanoscale*, 2019, **11**, 9563–9573.
39 A. Kamari, N. F. A. Aljafree and S. N. M. Yusoff, *Int. J. Biol. Macromol.*, 2016, **88**, 263–272.
40 T. Chuacharoen and C. M. Sabliov, *Colloids Surf., A*, 2016, **503**, 11–18.
41 C. G. da Rosa, M. V. de Oliveira Brisola Maciel, S. M. de Carvalho, A. P. Z. de Melo, B. Jummes, T. da Silva, S. M. Martelli, M. A. Villetti, F. C. Bertoldi and P. L. M. Barreto, *Colloids Surf., A*, 2015, **481**, 337–344.
42 E. M. Meijer, *Arch. Microbiol.*, 1978, **127**, 119–127.